1521-009X/48/11/1121–1128$35.00
Drug Metabolism and Disposition

https://doi.org/10.1124/dmd.120.000089
Drug Metab Dispos 48:1121–1128, November 2020

(–)-*N*-3-Benzylphenobarbital Is Superior to Omeprazole and (+)-*N*-3-Benzylnirvanol as a CYP2C19 Inhibitor in Suspended Human Hepatocytes[S]

Marie-Lynn Cuypers, Hugues Chanteux, Eric Gillent, Pierre Bonnaillie, Kenneth Saunders, Claire Beckers, Claude Delatour, Sylvie Dell'Aiera, Anna-Lena Ungell, and Johan Nicolaï

Pharmaceutical Sciences, KU Leuven, Leuven, Belgium (M.-L.C., C.B.) and Development Science, UCB Biopharma SRL, Braine-l'Alleud, Belgium (H.C., E.G., P.B., K.S., C.D., S.D., A.-L.U., J.N.)

Received April 20, 2020; accepted July 31, 2020

ABSTRACT

Early assessment of metabolism pathways of new chemical entities guides the understanding of drug-drug interactions. Selective enzyme inhibitors are indispensable in CYP reaction phenotyping. The most commonly applied CYP2C19 inhibitor, omeprazole, lacks selectivity. Two promising alternatives, (+)-*N*-3-benzylnirvanol and (−)-*N*-3-benzylphenobarbital, are already used as CYP2C19 inhibitors in some in vitro studies with suspended human hepatocytes. However, a full validation proving their suitability in terms of CYP and non-CYP selectivity has not been presented in literature. The present study provides a thorough comparison between omeprazole, (+)-*N*-3-benzylnirvanol, and (−)-*N*-3-benzylphenobarbital in terms of potency and selectivity and shows the superiority of (−)-*N*-3-benzylphenobarbital as a CYP2C19 inhibitor in suspended human hepatocytes. Furthermore, we evaluated the application of (−)-*N*-3-benzylphenobarbital to predict the in vivo contribution of CYP2C19 to drug metabolism [fraction metabolized (fm) of CYP2C19, $fm_{CYP2C19}$]. A set of 10 clinically used CYP2C19 substrates with reported in vivo $fm_{CYP2C19}$ data was evaluated. $fm_{CYP2C19}$, which was predicted using data from suspended human hepatocyte incubations, underestimated the in vivo $fm_{CYP2C19}$. The use of a different hepatocyte batch with a different CYP3A4/CYP2C19 activity ratio showed the impact of intrinsic CYP activities on the determination of $fm_{CYP2C19}$. Overall, this study confirms the selective CYP2C19 inhibition by (−)-*N*-3-benzylphenobarbital over other CYP isoforms (CYP1A2, CYP2B6, CYP2C8, CYP2C9, CYP2D6, and CYP3A4) and clinically relevant non-CYP enzymes [aldehyde oxidase, flavin-containing monooxygenase 3, N-acetyltransferase 2, uridine diphosphate glucuronosyltransferase (UGT) 1A1, UGT1A4, UGT2B7, UGT2B15] in suspended human hepatocytes. (−)-*N*-3-benzylphenobarbital is therefore the preferred CYP2C19 inhibitor to assess $fm_{CYP2C19}$ in suspended human hepatocytes in comparison with omeprazole and (+)-*N*-3-benzylnirvanol.

SIGNIFICANCE STATEMENT

(−)-*N*-3-Benzylphenobarbital is a more potent and selective inhibitor of CYP2C19 in suspended human hepatocytes than omeprazole and (+)-*N*-3-benzylnirvanol. (−)-*N*-3-Benzylphenobarbital can be used to predict the fraction metabolized by CYP2C19 in suspended human hepatocytes.

Introduction

CYP enzymes have been thoroughly investigated because they are responsible for the biotransformation of almost 80% of all commercially available drugs (Zanger and Schwab, 2013). CYP2C19 is one of the major enzymes in the human liver because it metabolizes ∼7% of the clinically used drugs, mostly anticonvulsants and antidepressants (Zanger and Schwab, 2013; FDA, 2020). Inhibitors, inducers, and genetic polymorphisms of CYP2C19 can influence the plasma levels of CYP2C19 substrates, resulting in a risk for toxic or subtherapeutic plasma levels. US Food and Drug Administration (FDA) guidelines recommend the assessment of these possible DDIs in the early stages of drug development (FDA, 2020). The evaluation of the fraction metabolized (fm) by a specific CYP enzyme (fm_{CYP}) in drug metabolism, CYP reaction phenotyping, plays an important role in predicting these DDIs. After all, fm_{CYP} influences the susceptibility of victim drugs toward inhibition or induction. Two methods are widely used for the quantitative determination of CYP enzyme involvement: 1) the use of chemicals, drugs, or antibodies as specific enzyme inhibitors in pooled human liver microsomes and 2) the use of individual human recombinant CYP enzymes (FDA, 2020).

A limitation of the systems suggested by the FDA is the use of human liver microsomes and recombinant enzymes. These in vitro systems are useful to obtain high levels of rare isoforms or to determine the role of one single enzyme in the metabolic profile (Parmentier et al., 2017). However, there are several disadvantages to using recombinant enzymes, namely 1) the evaluation of the cooperation between enzymes

Primary laboratory of origin: Development Sciences, UCB Biopharma SRL, Braine-l'Alleud, Belgium.
https://doi.org/10.1124/dmd.120.000089.
[S]This article has supplemental material available at dmd.aspetjournals.org.

ABBREVIATIONS: AO, aldehyde oxidase; Cl_{int}, intrinsic clearance; DDI, drug-drug interaction; FDA, US Food and Drug Administration; fm, fraction metabolized; FMO3, flavin-containing monooxygenase 3; HRMS, high-resolution mass spectrometry; IVIVC, in vitro–in vivo correlation; MS, mass spectrometry; m/z, mass-to-charge; NAT2, N-acetyltransferase 2; NCE, new chemical entity; RMSE, root-mean-square error; UGT, uridine diphosphate glucuronosyltransferase; UPLC, ultra-performance liquid chromatography; WGH, William's medium E containing 2 mM of glutamine and 15 mM of HEPES.

is impossible, 2) a relative activity factor is needed for scaling to in vivo, 3) enzymes are removed from their natural intracellular environment, and 4) the addition of cofactors is required (Brandon et al., 2003). Human liver microsomes are frequently used because of their low cost, high availability, ease of use, and high throughput (Lindmark et al., 2018). They represent a more advanced experimental model than recombinant enzymes, despite the fact that they also require the addition of cofactors and that they lack transporters or cell membranes as well as several key drug-metabolizing enzymes [e.g., sulfotransferase, aldehyde oxidase (AO), and xanthine oxidase]. This could result in higher relative contributions of CYP and uridine diphosphate glucuronosyltransferase (UGT) enzymes to drug metabolism as compared with the human in vivo situation (Brandon et al., 2003). The latter may result in an underestimation of the in vivo clearance of a drug product (Brown et al., 2007). Another problem that may arise when using human liver microsomes is the potential dependence of CYP enzyme activity on microsomal isolation (Nelson et al., 2001). Therefore, human hepatocytes are preferred for in vitro metabolic clearance experiments because they possess the full complement of phase I and phase II drug-metabolizing enzymes like sulfotransferase enzymes, AO, and xanthine oxidase (Brown et al., 2007). Human hepatocytes are cofactor self-sufficient, allow a simultaneous assessment of multiple enzymes/transporters, and better resemble the in vivo situation (Jiang et al., 2015; Lindmark et al., 2018). The ability to cryopreserve has helped to overcome the limited availability of human hepatocytes, contributing to the increasing popularity of human hepatocytes as an in vitro system to evaluate drug metabolism (Smith et al., 2012).

The availability of selective inhibitors is essential for predicting fm_{CYP} when using human hepatocytes. The most frequently used chemical inhibitor for CYP2C19 is omeprazole. However, omeprazole also inhibits CYP3A4, CYP2C9 (Ko et al., 1997), and UGT1A1 (Liu et al., 2011) in human liver microsomes and hepatocytes. In rare cases, this could result in an overprediction of the CYP2C19 contribution, potentially leading to unnecessary attrition of promising NCEs from the drug pipeline (Cai et al., 2004). Hence, researchers have looked for alternative CYP2C19 inhibitors to omeprazole. Several studies showed the CYP2C19 inhibitory potential of (+)-*N*-3-benzylnirvanol and (−)-*N*-3-benzylphenobarbital in human liver microsomes and their superiority over omeprazole (Suzuki et al., 2002; Cai et al., 2004). (−)-*N*-3-Benzylphenobarbital is already used in some in vitro suspended human hepatocyte studies (Kazmi et al., 2019), although a full validation in suspended human hepatocytes has presently not been published. Therefore, the current study investigated the potential of (−)-*N*-3-benzylphenobarbital and (+)-*N*-3-benzylnirvanol as CYP and non-CYP selective inhibitors of CYP2C19 in suspended human hepatocytes as alternatives to the nonselective CYP2C19 inhibitor omeprazole. Compounds with a wide range of $fm_{CYP2C19}$ were subsequently applied to validate the selected CYP2C19 inhibitor in suspended human hepatocytes to predict the in vivo $fm_{CYP2C19}$.

Materials and Methods

Materials

Cryopreserved human hepatocytes (mixed-sex pool of 20 donors, batch BSU) were obtained from BioreclamationIVT (Brussels, Belgium). Cryopreserved human hepatocytes with low CYP3A4 activity (mixed-sex pool of three donors, batch HUP182981) were obtained from Lonza (Walkersville, MD). (*S*)-(+)-Mephenytoin was purchased from Sigma-Aldrich (Saint Louis, MO) and Cayman Chemicals (Ann Arbor, MI). (−)-*N*-3-Benzylphenobarbital was synthesized at UCB Biopharma SRL (Braine-l'Alleud, Belgium). Midazolam was purchased from Apin Chemicals (Compton, Berkshire, UK). Omeprazole (racemic mixture), (+)-*N*-3-benzylnirvanol, glacial acetic acid, HEPES, DMSO, β-estradiol, sulfamethazine, citalopram, rabeprazole, lansoprazole, diazepam, phenytoin, naloxone, cimetidine, phenacetin, acetaminophen, bupropion, hydroxybupropion, diclofenac, 4-hydroxydiclofenac, dextromethorphan, dextrorphan, rosiglitazone, 5-hydroxyrosiglitazone, 1-hydroxymidazolam, carbazeran, 4-hydroxycarbazeran, 4-hydroxymephenytoin, and internal standards used in the bioanalysis (acetaminophen-D_4, hydroxybupropion-D_6, 1-hydroxymidazolam-D_4, 4-hydroxydiclofenac-$^{13}C_6$, 4-hydroxymephenytoin-D_3, dextrorphan-D_3, and 5-hydroxyrosiglitazone-D_4) were obtained from Sigma-Aldrich. Trifluoperazine, pantoprazole, clopidogrel, labetalol, and moclobemide were acquired from Cayman Chemicals. Clobazam, norclobazam, and oxazepam were provided by LGC (Teddington, Middlesex, UK). William's medium E was purchased from Lonza (Verviers, Belgium). Glutamine, cryopreserved hepatocyte recovery medium, and trypan blue 0.4% were obtained from Thermo Fisher Scientific (Waltham, MA). Glucuronidase/arylsulfatase was bought from Roche (Vilvoorde, Belgium). Ammonium acetate was purchased from Merck (Darmstadt, Germany). Ultra-performance liquid chromatography (UPLC)-grade water, acetonitrile, methanol, ethanol, formic acid, and trifluoroacetic acid were obtained from Biosolve (Valkenswaard, The Netherlands).

Methods

Thawing of Cryopreserved Human Hepatocytes. On the day of the experiment, vials of human hepatocytes were taken out of the cryoconservator. The vials were submerged in a water bath (37°C) and gently shaken until the ice was almost completely thawed (1 to 2 minutes). The content of the vials was transferred into a falcon tube containing 50 ml of cryopreserved hepatocyte recovery medium, and the vial was rinsed with cryopreserved hepatocyte recovery medium (37°C). The falcon tube containing the hepatocytes was centrifuged for 10 minutes (21°C, 100*g*) (4-16KS; Sigma, Osterode am Harz, Germany). The supernatant was removed, and the pellet of hepatocytes was gently loosened by tapping. Two milliliters per vial of William's medium E containing 2 mM of glutamine and 15 mM of HEPES (WGH) was added to the falcon tube. A 100-μl aliquot of the hepatocyte suspension was added to 100 μl trypan blue (0.4%), and cells were counted using a hemocytometer. Viability was determined based on trypan blue exclusion (always >84.4%). The hepatocytes were diluted with WGH to the required concentration and were transferred into the wells of a 48-well plate.

Incubations with Suspended Human Hepatocytes. The hepatocytes (2×10^6 cells/ml) were preincubated for 30 minutes in a humidified incubator (5% CO_2, 37°C). During the experiment, the hepatocytes were kept in suspension using agitation (Titramax 100, 450 rpm). The reaction was initiated by adding one volume of prewarmed (37°C) WGH containing substrates and inhibitors or inhibitors alone when a 3-hour preincubation period with only inhibitors was required. Final concentrations of DMSO and acetonitrile in incubates were ≤0.05% and ≤1%, respectively. After a 30-minute incubation time, the reaction was stopped by adding one volume of sample to two volumes of ice-cold acetonitrile in a 96–deep well plate. The plate was centrifuged (15 minutes, 4°C, at 2908*g*) (4-16KS; Sigma), and the clear supernatant was analyzed by UPLC–mass spectrometry (MS)/MS. For rosiglitazone samples, the obtained supernatant was evaporated under a stream of nitrogen gas, and the residue was redissolved in 100 μl acetate buffer (50 mM, pH 5.0) containing glucuronidase (0.358 U/ml) and arylsulfatase (0.48 U/ml). An extra 1-hour incubation (37°C) was carried out to convert the glucuronide and sulfate metabolites back to 5-hydroxyrosiglitazone. The reaction was stopped by adding one volume of sample to two volumes of ice-cold acetonitrile in a 96–deep well plate. The plate was centrifuged (15 minutes, 4°C, at 2908*g*) (4-16KS; Sigma), and the clear supernatant was used for UPLC-MS/MS analysis. The final concentration of (*S*)-(+)-mephenytoin, the CYP2C19 substrate, was 5 μM. A range of final inhibitor concentrations was used to assess their CYP2C19 inhibition potential: omeprazole (0, 0.06, 0.2, 2, 6, 20, and 60 μM), (+)-*N*-3-benzylnirvanol (0, 0.01, 0.03, 0.1, 0.3, 1, 3, 10, and 30 μM), and (−)-*N*-3-benzylphenobarbital (0.003, 0.01, 0.03, 0.1, 0.3, 1, 3, and 10 μM).

The effects of omeprazole (final concentration: 20 μM), (+)-*N*-3-benzylnirvanol (final concentration: 10 μM), and (−)-*N*-3-benzylphenobarbital (final concentration: 1 μM) on the activity of major CYP enzymes (CYP1A2, CYP2B6, CYP2C8, CYP2C9, CYP2C19, CYP2D6, CYP3A4) and AO were evaluated without and with a 3-hour preincubation period in presence of the inhibitors. Two in-house validated CYP substrate cocktails were used for the incubation of probe substrates, except rosiglitazone and carbazeran (Gerin et al., 2013). Probe substrates were incubated at concentrations close to the K_m value of the probe substrate reaction of interest. Supplemental Table 1 provides an overview of the

different probe substrate reactions, the final substrate concentrations, and the cocktail compositions.

For (−)-*N*-3-benzylphenobarbital, selectivity against clinically relevant non-CYP enzymes was also evaluated. Specific metabolite formation was followed for estradiol (UGT1A1), trifluoperazine (UGT1A4), naloxone (UGT2B7), oxazepam (UGT2B15), sulfamethazine [N-acetyltransferase 2 (NAT2)], cimetidine [flavin-containing monooxygenase 3 (FMO3)], and carbazeran (AO, described above) in presence and absence of (−)-*N*-3-benzylphenobarbital (1 μM) in suspended human hepatocytes (1×10^6 cells/ml). Probe substrates were incubated at a final concentration of 0.5 μM, except 2 μM was used for cimetidine. Reactions were stopped at six different time points (0, 10, 30, 60, 120, and 240 minutes) by adding one volume of sample to one volume of ice-cold acetonitrile. Plates were centrifuged (15 minutes, 4°C, at 2908*g*) (4-16KS; Sigma), and the clear supernatant was diluted with two volumes of UPLC-grade water before analysis by UPLC–high-resolution mass spectrometry (HRMS).

An in vitro–in vivo correlation (IVIVC) of $fm_{CYP2C19}$ was based on incubations of a set of clinically used known CYP2C19 substrates [phenytoin, diazepam, clobazam, norclobazam, citalopram, moclobemide, rabeprazole, lansoprazole, pantoprazole, omeprazole, labetalol, and (*S*)-(+)-mephenytoin] incubated at a final concentration of 0.5 μM, except 10 μM was used for clobazam and norclobazam, and 0.005 μM was used for omeprazole. Incubations were carried out in the presence and absence of (−)-*N*-3-benzylphenobarbital (1 μM). Reactions were stopped at six different time points (0, 30, 60, 120, 180, and 240 minutes) by adding one volume of sample to one volume of ice-cold acetonitrile. Parent depletion was followed in 6-fold–diluted supernatant (UPLC-grade water) by UPLC-MS/MS for rabeprazole, lansoprazole, pantoprazole, omeprazole, labetalol, and (*S*)-(+)-mephenytoin samples. Threefold-diluted supernatant (UPLC-grade water) of phenytoin, diazepam, clobazam, norclobazam, citalopram, and moclobemide was analyzed by UPLC-HRMS to monitor metabolite formation.

Analytical Methods.

UPLC-MS/MS methods to monitor metabolite formation. Two CYP substrate cocktail methods were used to analyze the metabolites of CYP probe substrates. Cocktail 1 refers to the analytical method used to quantify acetaminophen, 4-hydroxybupropion, 4-hydroxydiclofenac, and 1-hydroxymidazolam (Gerin et al., 2013), and cocktail 2 refers to the analytical method used to quantify 4-hydroxymephenytoin and dextrorphan.

Cocktail 1. One volume of internal standard solution (acetaminophen-D_4, hydroxybupropion-D_6, 1-hydroxymidazolam-D_4, 4-hydroxydiclofenac-$^{13}C_6$) was added to five volumes of the 3-fold–diluted supernatant. Samples were analyzed on an Agilent 1290 UPLC system (Agilent Technologies Santa Clara, CA) coupled to a Sciex API 5000 mass spectrometer (Applied Biosystems, Mississauga, Canada) operated in positive ion mode. Chromatographic separation was obtained using gradient elution and a Zorbax Eclipse plus XDB C18 (50 × 2.1 mm, 1.8 μm) column operated at 40°C. The injection volume was 4 μl, and the flow rate was 0.350 ml/min. Gradient elution with mobile phase A (H_2O with 0.1% trifluoroacetic acid at pH 2.4) and mobile phase B (acetonitrile) started at 95% A (2.16 minutes); decreased, respectively, to 75% A in 0.24 minutes, 60% A in 1.46 minutes, 50% A in 0.01 minutes, 20% (0.49 minutes) in 0.47 minutes, 10% A (0.72 minutes) in 0.01 minutes; and finally returned to its initial condition of 95% A (0.93 minutes). Data acquisition and system control were performed by Analyst 6.1 software. Mass-to-charge (m/z) transitions are listed in Supplemental Table 2. Concentrations were calculated from peak area ratios based on a calibration curve with 10 different concentrations. Three quality-control samples were analyzed for the qualification of the analysis.

Cocktail 2 and rosiglitazone/carbazeran. Cocktail 2 [(*S*)-(+)-mephenytoin and dextromethorphan], rosiglitazone, and carbazeran samples were incubated separately and analyzed by the same UPLC method. For cocktail 2 and rosiglitazone samples, one volume of internal standard solution (4-hydroxymephenytoin-D_3, dextrorphan-D_3, 5-hydroxyrosiglitazone-D_4) was added to one volume of supernatant. The plate was evaporated under a stream of nitrogen gas at 50°C. The residue was redissolved in 100 μl H_2O:acetonitrile:formic acid (90:10:0.1, v/v/v). For carbazeran samples, two volumes of internal standard solution (dextromethorphan) were added to one volume of supernatant, and no evaporation step was needed. All samples were analyzed on a Shimadzu Nexera X2 UPLC system (Shimadzu, Kyoto, Japan) coupled to a Sciex API 5000 mass spectrometer (Applied Biosystems) operated in positive ion mode. Chromatographic separation was obtained using gradient elution and a Zorbax Eclipse plus XDB C18 (50 × 2.1 mm, 1.8 μm) column operated at 30°C. The injection volume was 5 μl, and the flow rate was 0.350 ml/min. Gradient elution with mobile phase A (H_2O with 0.1% formic acid) and mobile phase B (methanol with 0.1% formic acid) started at 95% A (1 minute), and, respectively, decreased to 80% A (0.5 minutes) in 1.5 minutes, 20% A in 3 minutes, 10% A (0.98 minutes) in 0.01 minutes, and 5% A (1 minute) in 0.01 minutes. Data acquisition and system control were performed by Analyst 6.1 software. The m/z transitions are listed in Supplemental Table 2. Concentrations were calculated using peak area ratios and a calibration curve with eight different concentrations. Three quality-control samples were analyzed for the qualification of the analysis. The cocktail was validated internally, showing no interaction between substrates (unpublished data).

UPLC-MS/MS method to monitor parent drug disappearance. Parent drug disappearance was measured for six CYP2C19 substrates (rabeprazole, lansoprazole, pantoprazole, omeprazole, labetalol, and (*S*)-(+)-mephenytoin) to determine the $fm_{CYP2C19}$ in suspended human hepatocytes. The 6-fold–diluted samples were analyzed on a Shimadzu Nexera X2 UPLC system (Shimadzu) coupled to a Sciex API 5000 mass spectrometer (Applied Biosystems) operated in positive ion mode, except for when negative ion mode was used for (*S*)-(+)-mephenytoin samples. Chromatographic separation was obtained using gradient elution and an Acquity HSS T3 C18 (50 × 2.1 mm, 1.8 μm) column operated at 40°C. The injection volume and the flow rate were 5 μl and 0.7 ml/min, respectively. Gradient elution with mobile phase A (ammonium acetate 10 mM with 0.1% acetic acid) and mobile phase B (acetonitrile) started at 90% A (0.30 minutes) and decreased, respectively, to 30% A in 3.70 minutes and 5% A in 1 minute and finally returned to its initial condition of 90% A. Data acquisition and system control were performed by Analyst 6.1 software. The m/z transitions are listed in Supplemental Table 2.

UPLC-HRMS method to monitor metabolite formation. Twofold-diluted supernatant of incubations performed with citalopram, clobazam, diazepam, moclobemide, norclobazam, phenytoin, β-estradiol, trifluoperazine, naloxone, oxazepam, sulfamethazine, and cimetidine samples was analyzed by UPLC-HRMS to detect specific metabolites. Samples were analyzed on an Acquity UPLC instrument (Waters, Manchester, UK) coupled to a XevoG2S Qtof high-resolution mass spectrometer (Waters) operated in positive ion mode, except for when negative ion mode was used for β-estradiol samples or when coupled to a VION ion mobility quadrupole time-of-flight high-resolution mass spectrometer for sulfamethazine samples. Citalopram, clobazam, clopidogrel, diazepam, moclobemide, norclobazam, trifluoperazine, and oxazepam samples were analyzed on a Waters CSH column (100 × 2.1 mm, 1.7 μm). Injection volume and flow rate were 2 μl and 3 μl/min, respectively. A Waters HSS C18 (100 × 2.1 mm, 1.7 μm) column was used for analyzing β-estradiol, naloxone, and cimetidine samples. Injection volume and flow rate were 7 μl and 400 μl/min, respectively. Chromatographic separation was obtained using gradient elution with mobile phase A (ammonium acetate 10 mM:acetic acid 0.1%) and mobile phase B (acetonitrile) starting at 90% A (1 minute), decreased to 10% A (10.5 minute) in 9 minutes, and returned to its initial conditions in 10.51 minutes. Chromatographic separation for sulfamethazine samples was obtained using gradient elution and a Waters HSS C18 column (100 × 0.3 mm, 1.7 μm). Injection volume and flow rate were 2 μl and 7.5 μl/min, respectively. Gradient elution with mobile phase A (H_2O:formic acid 0,1%) and mobile phase B (acetonitrile:formic acid 0,1%) started at 95% (1 minute) A, decreased to 10% A in 8 minutes (1.5 minute), and finally increased to 90% A in 0.01 minutes. Full scan MS-MS data were acquired using Masslynx V4.1 SCN884.

Data Analysis. The rate of metabolite formation (picomoles per minute per million cells) was calculated using eq. 1, in which [*metabolite*] is the concentration of metabolite formed in micromolars, *t* is the time of incubation in minutes, and [*hepatocytes*] is the hepatocyte concentration in the incubate in million cells/ml.

$$v = \frac{[metabolite] \cdot 1000}{t \cdot [hepatocytes]} \quad (1)$$

IC_{50} values were determined with GraphPad Prism 7.04 from GraphPad software (San Diego, CA) using nonlinear regression four-parameter variable slope analysis (eq. 2) (GraphPad, 2020). All results were based on the least-squares fit.

$$Metabolite\ formation\ (\%\ of\ control) = \frac{100}{1 + 10^{((\log IC_{50} - \log[I]) \cdot HillSlope)}} \quad (2)$$

In which IC_{50} (micromolars) is the concentration of inhibitor resulting in 50% inhibition of the metabolite formation (% of control), the logarithm of the inhibitor concentration (log[*I*]) is the × variable, and *Hillslope* describes the steepness of the curves.

The in vitro intrinsic clearance (Cl_{int}) (microliter per minute per million cells) was calculated using the in vitro half-life ($t_{1/2}$) (minutes) of compound disappearance (eq. 3) (Obach et al., 1997).

$$Cl_{int} = -\frac{0.693 \cdot 1000}{t_{1/2} \cdot [hepatocytes]} \quad (3)$$

For low-turnover compounds, the intrinsic clearance (microliter per minute per million cells) was estimated based on metabolite formation rate. The metabolite formation rate was obtained by measuring the slope of the sum of the normalized peak areas (normalized for parent peak area) of the detected metabolites over time (eq. 4).

$$Cl_{int} = \frac{Slope\ (normalized\ peak\ area\ over\ time) \cdot 1000}{[Hepatocytes]} \quad (4)$$

The percentage inhibition (*% inhibition*) of metabolite formation, which is used for assessing inhibitor selectivity in suspended human hepatocytes, was measured by comparing the metabolite concentrations (micromolars) or peak areas in samples with inhibitor ($[metabolite]_{inhibitor}$, $Peak\ area_{inhibitor}$) and control ($[metabolite]_{control}$, $Peak\ area_{control}$) samples (eq. 5). For the IVIVC, the predicted fm_{CYP} values in suspended human hepatocytes were calculated using eq. 6. Cl_{int} values applied in eq. 6 were obtained using the ratio of parent drug clearance (eq. 3) or metabolite formation (eq. 4) in the absence ($Cl_{int\_control}$) and presence ($Cl_{int\_inhibitor}$) of (−)-*N*-3-benzylphenobarbital.

$$\begin{aligned} \%\ inhibition &= \left(1 - \frac{[metabolite]_{inhibitor}}{[metabolite]_{control}}\right) \cdot 100\% \\ &= \left(1 - \frac{Peak\ area_{inhibitor}}{Peak\ area_{control}}\right) \cdot 100\% \end{aligned} \quad (5)$$

$$Fm_{CYP2C19} = 1 - \frac{Cl_{int\_inhibitor}}{Cl_{int\_control}} \quad (6)$$

Statistical Analysis

To study the relationship between the in vitro and in vivo $fm_{CYP2C19}$, a simple linear regression was performed. The linear correlation was evaluated using the *RMSE* (eq. 7) (Chai and Draxler, 2014), in which $\hat{y}_i$ is the predicted value, y_i is the observed value, and n is the number of data points.

$$RMSE = \sqrt{\frac{1}{n}\sum_i (\hat{y} - y_i)^2} \quad (7)$$

Results

Assessment of the Inhibitory Potential of Omeprazole, (+)-*N*-3-Benzylnirvanol, and (−)-*N*-3-Benzylphenobarbital against CYP2C19. Optimal conditions were selected in terms of incubation time and hepatocyte concentration to ensure that metabolite formation was determined in the linear range, and a probe substrate concentration below the K_m was selected to avoid saturation conditions (unpublished data). Inhibitory potentials of omeprazole, (+)-*N*-3-benzylnirvanol, and (−)-*N*-3-benzylphenobarbital against CYP2C19-mediated formation of 4-hydroxymephenytoin from *S*-(+)-mephenytoin (5 μM) were evaluated by comparing IC_{50} values without and with a 3-hour preincubation in presence of the inhibitor in suspended human hepatocytes (Fig. 1; Table 1). The IC_{50} of omeprazole was 1.7 μM. After increasing the preincubation time, an IC_{50} shift was observed from 1.7 to 0.2 μM (+). The IC_{50} of *N*-3-benzylnirvanol valued 0.2 μM and increased to 1.6 μM after a 3-hour preincubation. The most potent inhibitor of CYP2C19 was (−)-*N*-3-benzylphenobarbital with an IC_{50} value of 0.09 μM without preincubation and 0.2 μM after a 3-hour inhibitor preincubation. Based on the IC_{90} (inhibitor concentration that gives 90% of the maximum inhibition), concentrations of 20 μM (omeprazole), 10 μM [(+)-*N*-3-benzylnirvanol], and 1 μM [(−)-*N*-3-benzylphenobarbital] were selected for further evaluation.

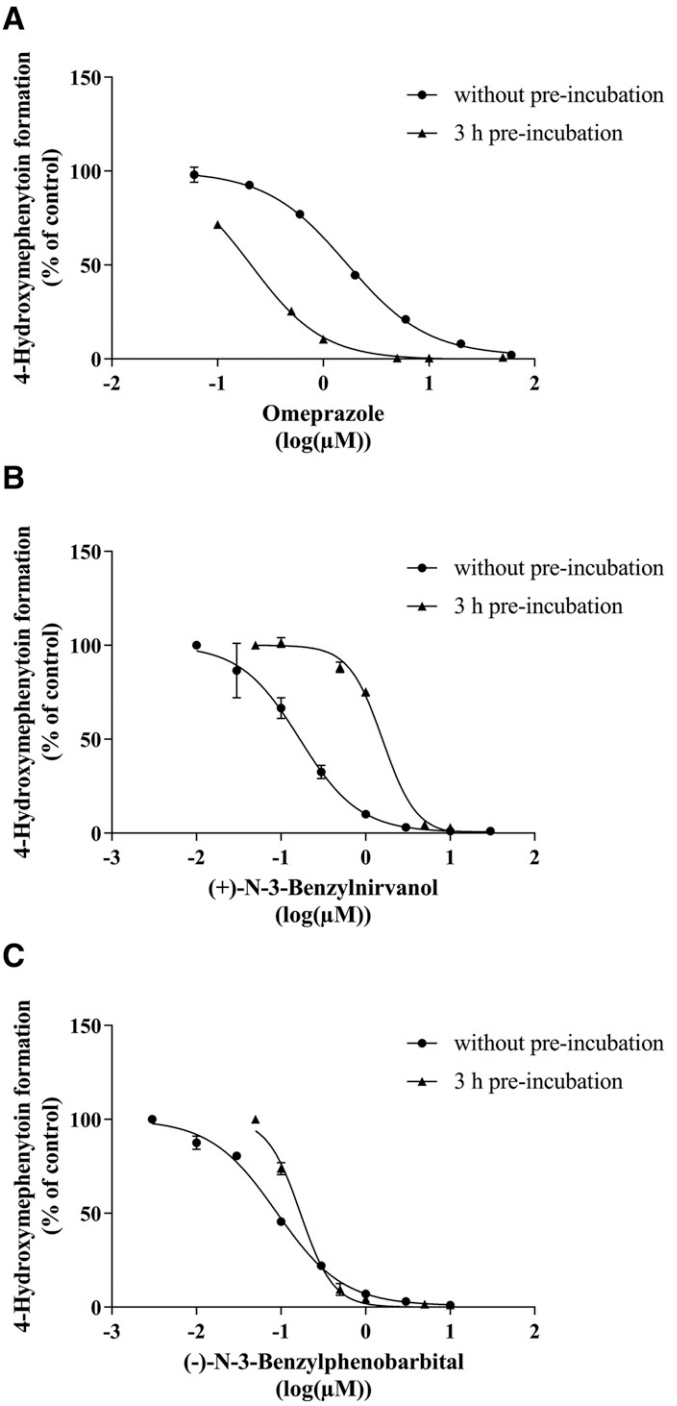

Fig. 1. Inhibition profiles for the effect of omeprazole (A), (+)-*N*-3-benzylnirvanol (B), and (−)-*N*-3-benzylphenobarbital (C) on the formation of 4-hydroxymephenytoin from (*S*)-(+)-mephenytoin (5 μM) in suspended human hepatocytes (1 × 10^6 cells/ml) (BSU) without (•) and after a 3-hour (▲) inhibitor preincubation. Points represent mean experimental data from two experiments in singlicate ± variation (n = 2). Lines represent nonlinear regression results for four-parameter fits calculated with GraphPad Prism 7.04 from GraphPad software.

TABLE 1

Experimentally determined mean IC_{50} values (two experiments in singlicate, $n = 2$) of omeprazole, (+)-*N*-3-benzylnirvanol, and (−)-*N*-3-benzylphenobarbital on 4-hydroxymephenytoin formation from (*S*)-(+)-mephenytoin (5 μM) in suspended human hepatocytes (1×10^6 cells/ml) (BSU) without and after 3-h inhibitor preincubation

	IC_{50} (μM) without Preincubation	IC_{50} with Preincubation
Omeprazole	1.67	0.209
(+)-*N*-3-Benzylnirvanol	0.166	1.592
(−)-*N*-3-Benzylphenobarbital	0.0892	0.169

Evaluation of the Selectivity of Omeprazole, (+)-*N*-3-Benzylnirvanol, and (−)-*N*-3-Benzylphenobarbital toward CYP2C19. To evaluate the selectivity of omeprazole, (+)-*N*-3-benzylnirvanol, and (−)-*N*-3-benzylphenobarbital toward CYP2C19, their inhibitory effect on major CYP enzymes and AO was assessed after probe substrate reactions: phenacetin *O*-deethylation (CYP1A2), bupropion 4-hydroxylation (CYP2B6), rosiglitazone 5-hydroxylation (CYP2C8), diclofenac 4-hydroxylation (CYP2C9), (*S*)-(+)-mephenytoin 4-hydroxylation (CYP2C19), dextromethorphan *O*-demethylation (CYP2D6), midazolam 1-hydroxylation (CYP3A4), and carbazeran 4-hydroxylation (AO) in suspended human hepatocytes (1×10^6 cells/ml). Selectivity against other clinically relevant non-CYP enzymes was evaluated for (−)-*N*-3-benzylphenobarbital. For that purpose, specific metabolite formation was followed for estradiol (UGT1A1), trifluoperazine (UGT1A4), naloxone (UGT2B7), oxazepam (UGT2B15), sulfamethazine (NAT2), and cimetidine (FMO3).

The data showed that (−)-*N*-3-benzylphenobarbital (1 μM) was the most selective inhibitor of CYP2C19. For all CYP enzymes tested, inhibition remained below 20%, with and without inhibitor preincubation (Fig. 2; Table 2). In contrast, omeprazole (20 μM) was not as selective since it also affected CYP1A2 (26% inhibition) and CYP2C9 (34% inhibition) (Fig. 2). (+)-*N*-3-Benzylnirvanol (10 μM) also showed not to be selective toward CYP2C19. It significantly inhibited CYP1A2 (49%), and after inhibitor preincubation, it also impacted CYP2B6 (43%), CYP2C8 (31%), and CYP3A4 (47%) activity (Fig. 2).

Because (−)-*N*-3-benzylphenobarbital was the most promising CYP2C19 inhibitor based on CYP selectivity, its selectivity against some important non-CYP enzymes was evaluated. (−)-*N*-3-Benzylphenobarbital (1 μM) caused less than 10% inhibition of the evaluated non-CYP enzymes AO (0.0%), UGT1A1 (7.3%), UGT1A4 (−6.7%), UGT2B7 (−8.2%), UGT2B15 (1.1%), NAT2 (0.8%), and FMO3 (−11.7%) (Fig. 3; Table 2).

IVIVC of $fm_{CYP2C19}$. To evaluate the use of (−)-*N*-3-benzylphenobarbital as an in vitro tool to predict $fm_{CYP2C19}$, the effect of (−)-*N*-3-benzylphenobarbital (1 μM) on the intrinsic clearance of a set of clinically used CYP2C19 substrates, with reported in vivo $fm_{CYP2C19}$ data, was evaluated in suspended human hepatocytes.

The use of the BSU hepatocyte batch demonstrated some trend of $fm_{CYP2C19}$ underprediction (*RMSE* = 0.12) (Table 3). A potential hypothesis is that the intrinsic activity ratio of CYP2C19 against CYP3A4 in the BSU batch is too low to be relevant. This hypothesis was tested by using a hepatocyte batch (HUP182981) with a 10-fold–lower CYP3A4 activity and similar activities for other main CYP enzymes (Supplemental Table 3). Results showed the impact of intrinsic CYP activities on the fm determination (*RMSE* = 0.11) (Fig. 4). Additional work is warranted to further identify an optimal human hepatocyte batch for phenotyping purposes. But overall, (−)-*N*-3-benzylphenobarbital is the most appropriate CYP2C19 inhibitor to determine CYP2C19 contribution in the metabolism of NCEs. Table 3

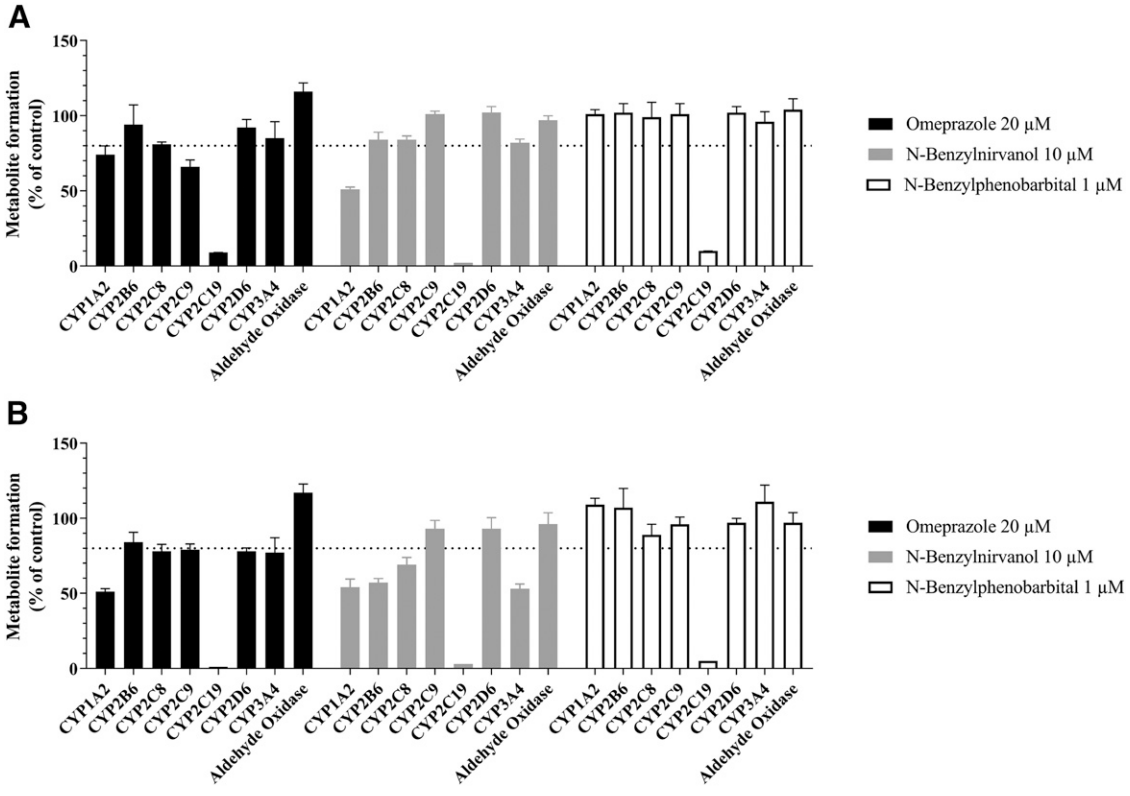

Fig. 2. Effect of omeprazole (20 μM), (+)-*N*-3-benzylnirvanol (10 μM), and (−)-*N*-3-benzylphenobarbital (1 μM) on major CYP enzymes (1A2, 2B6, 2C8, 2C9, 2C19, 2D6, 3A4) and AO in suspended human hepatocytes (1×10^6 cells/ml) (BSU) without (A) and after a 3-hour (B) inhibitor preincubation. Bars represent mean values ± S.D. (two experiments in triplicate, $n = 6$). The dotted line represents 20% inhibition.

TABLE 2

Mean percentage inhibition (two experiments performed in triplicate, $n = 6$) ± S.D. of enzyme activity by (−)-*N*-3-benzylphenobarbital (1 μM) in suspended human hepatocytes (1×10^6 cells/ml) (BSU) without and after a 3-h inhibitor preincubation

Substrate	Enzyme	% Inhibition $_{30\ min}$ preincubation	% Inhibition $_{3\ h}$ preincubation
Carbazeran	AO	−4.0 ± 7.1	3.1 ± 6.7
Phenacetin	CYP1A2	−0.6 ± 2.7	−9.4 ± 3.5
Bupropion	CYP2B6	−2.4 ± 6.4	−6.9 ± 12.2
Rosiglitazone	CYP2C8	0.5 ± 10.4	10.9 ± 8.3
Diclofenac	CYP2C9	−0.6 ± 6.9	4.4 ± 4.7
(*S*)-(+)-Mephenytoin	CYP2C19	89.9 ± 0.8	94.7 ± 0.5
Dextromethorphan	CYP2D6	−2.5 ± 3.8	2.6 ± 3.3
Midazolam	CYP3A4	3.5 ± 6.6	−11.0 ± 10.0
Cimetidine	FMO3	−11.7[a]	/
Sulfamethazine	NAT2	0.7[a]	/
β-Estradiol	UGT1A1	7.3[a]	/
Trifluoperazine	UGT1A4	−6.8[a]	/
Oxazepam	UGT2B15	1.1[a]	/
Naloxone	UGT2B7	−8.2[a]	/

[a]Mean percentage inhibition (results from a single experiment performed in singlicate, $n = 1$).

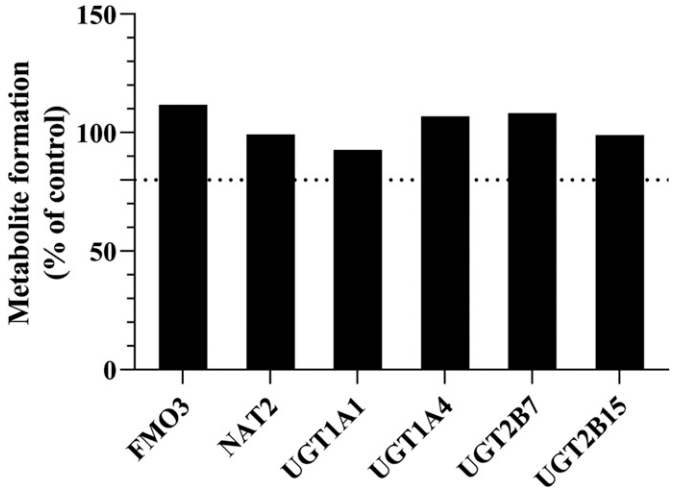

Fig. 3. Effect of (−)-*N*-3-benzylphenobarbital (1 μM) on major non-CYP enzymes (FMO3, NAT2, UGT1A1, UGT1A4, UGT2B7, UGT2B15) in suspended human hepatocytes (1×10^6 cells/ml) (BSU). Bars represent values from one single experiment performed in singlicate. The dotted line represents 20% inhibition.

provides an overview of the Cl_{int} (HUP182981) together with the predicted and observed $fm_{CYP2C19}$ for the tested compounds.

Discussion

FDA guidelines on drug interactions have aided in routinizing the in vitro evaluation of the DDI potential of NCEs, decreasing late-stage attrition due to unacceptable pharmacokinetics in the presence of coadministered drugs. These guidelines cover 1) the understanding of the major elimination pathways of NCEs, 2) evaluation of the effect of NCEs on different metabolic enzymes, and 3) estimation of the involvement of different enzymes and transporters in the disposition of the NCEs (FDA, 2020). The FDA recommends applying at least two of the following methods for reaction phenotyping to avoid false positive/negative prediction of DDIs: 1) the use of chemicals, drugs, or antibodies as specific enzyme inhibitors in pooled human liver microsomes or 2) the use of individual human recombinant CYP enzymes (FDA, 2020). The fraction of metabolic clearance (part of the total drug clearance mediated by drug metabolism, $f_{Cl\_metabolism}$) and the fraction metabolized by a specific enzyme (fraction of the drug metabolism mediated by a specific enzyme, fm_{CYP}) are key parameters in DDI prediction. An exponential increase of the victim drug's area-under-the-curve ratio with fm_{CYP} is observed when $f_{Cl\_metabolism} \times fm_{CYP}$ exceeds 0.5. This is associated with an increased risk for toxic drug exposure after coadministration of the drug of interest with a perpetrator for DDI (Bohnert et al., 2016).

Selective and potent chemical inhibitors are available for most major CYP enzymes apart from CYP2C19. Omeprazole, the most commonly used in vitro CYP2C19 inhibitor, also inhibits CYP3A4, CYP2C9 (Cai et al., 2004), and UGT1A1 (Liu et al., 2011). Another commonly used and time-dependent inhibitor of CYP2C19, ticlopidine, is also a potent inhibitor of CYP2D6 and CYP2B6 (Khojasteh et al., 2011). In addition to omeprazole and ticlopidine, there are several other non-selective CYP2C19 inhibitors (nootkatone, tranylcypromine, norfluoxetine) (Suzuki et al., 2002; Cai et al., 2004; Khojasteh et al., 2011). The discovery of (+)-*N*-3-benylnirvanol and (−)-*N*-3-benzylphenobarbital brought two promising alternative CYP2C19 inhibitors forward. Recombinant enzyme and microsomal data indicated that (−)-*N*-3-benzylphenobarbital and (+)-*N*-3-benzylnirvanol are potent CYP2C19 inhibitors, with (−)-*N*-3-benzylphenobarbital showing greater selectivity toward CYP2C19 as compared with omeprazole (Suzuki et al., 2002; Cai et al., 2004). However, a full validation on the use of these novel CYP2C19 inhibitors in suspended human hepatocytes had not been reported. Therefore, the present study compared omeprazole, (+)-*N*-3-benzylnirvanol, and (−)-*N*-3-benzylphenobarbital as potent and selective inhibitors of CYP2C19 and aimed to characterize (−)-*N*-3-benzylphenobarbital as a tool for $fm_{CYP2C19}$ estimation in suspended human hepatocytes.

We found that in comparison with omeprazole and (+)-*N*-3-benzylnirvanol, (−)-*N*-3-benzylphenobarbital showed to be the most potent inhibitor of CYP2C19 in suspended human hepatocytes. The observed IC_{50} value for (−)-*N*-3-benzylphenobarbital was 2-fold lower than reported for human liver microsomes. Potentially, this is related to differences in protein binding in these in vitro systems (Cai et al., 2004). Since suspended human hepatocyte experiments can last up to 4 hours, the inhibition of CYP2C19 over the entire time course of the experiment must be ensured (Smith et al., 2012). Therefore, additional inhibition experiments including a 3-hour inhibitor preincubation were carried out to select the appropriate inhibitor concentrations. Preincubation of the inhibitors resulted in a decrease of the IC_{50} of omeprazole for CYP2C19, pointing toward time-dependent inhibition (Shirasaka et al., 2013). An increase of the IC_{50} of (+)-*N*-3-benzylnirvanol was potentially caused by metabolic instability of the inhibitor itself. The IC_{50} of (−)-*N*-3-benzylphenobarbital toward CYP2C19 remained within 2-fold after a 3-hour preincubation of the inhibitor.

Selectivity of the currently tested inhibitors toward CYP2C19 was evaluated in comparison with major CYP enzymes CYP1A2, CYP2B6, CYP2C8, CYP2C9, CYP2D6, and CYP3A4. (−)-*N*-3-Benzylphenobarbital (1 μM) did not cause more than 20% inhibition of these enzymes (without and after a 3-hour preincubation). These human hepatocyte data confirm the findings by Cai et al. (2004), which advocated the great selectivity of (−)-*N*-3-benzylphenobarbital in human liver microsomes (Cai et al., 2004). Their study did show a 25% inhibition of CYP2C9 at a (−)-*N*-3-benzylphenobarbital concentration of 6.25 μM. However, this is not relevant to the current study because such high concentrations are not needed to achieve over 90% inhibition of CYP2C19 in suspended human hepatocytes. In contrast, omeprazole (20 μM) inhibited CYP1A2 (26%) and CYP2C9 (34%) and, to a lesser extent, CYP2C8 (19%), CYP2D6 (8%), and CYP3A4 (15%). A previous study by Ko et al. (1997) demonstrated the inhibition potential of omeprazole for CYP2C9. Yet no inhibition

TABLE 3

Determination of CYP2C19 contribution to the metabolic clearance, based on parent depletion or metabolite formation (*), obtained in suspended human hepatocytes (1 × 10^6 cells/ml) (BSU and HUP182981) for 10 marketed drugs using (−)-*N*-3-benzylphenobarbital (1 μM)

In vitro $fm_{CYP2C19}$ values from a single experiment calculated using eq. 6.

Compound	$fm_{CYP2C19}$ (%)			Reference
	In Vitro *BSU*	In Vitro HUP182981	In Vivo (Observed)	
Rabeprazole	27.9	24.9	16	Sakai et al., 2001
Phenytoin*	6.45	10.9	20	Patsalos, 2013
Clobazam*	18.1	31.1	21	Walzer et al., 2012
Diazepam*	25.7	44.2	43	Sohn et al., 1992
Labetalol	36.6	39.0	66	Chan et al., 2013
Norclobazam*	67.5	74.9	68	Walzer et al., 2012
Lansoprazole	47.2	61.2	73	Sakai et al., 2001
Pantoprazole	74.6	71.9	83	Tanaka et al., 1997
Omeprazole	71.0	76.8	86	Sakai et al., 2001
(*S*)-(+)-Mephenytoin	88.9	77.9	90	Yao et al., 2003

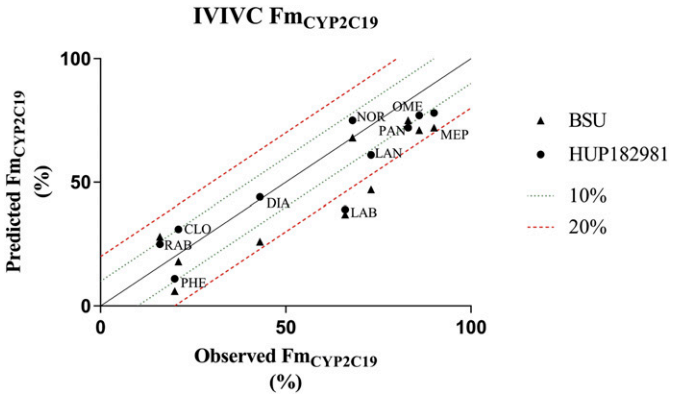

Fig. 4. IVIVC between observed in vivo (literature) and $fm_{CYP2C19}$ predicted from in vitro incubations. Points represent data from one experiment and two different hepatocyte batches: BSU (▲), HUP182981 (•). Dotted lines indicate 10% (green) and dashed line 20% (red) absolute error. CLO, clobazam; DIA, diazepam; LAB, labetalol; LAN, lansoprazole; MEP, (S)-(+)-mephenytoin; NOR, norclobazam; OME, omeprazole; PAN, pantoprazole; PHE, phenytoin; RAB, rabeprazole.

against CYP1A2 was observed by Ko et al. (1997), which could be explained by the lower concentrations of omeprazole applied in their study (1–5 μM) (Ko et al., 1997). Also, (+)-*N*-3-benzylnirvanol (10 μM) inhibited all the evaluated CYP enzymes except CYP2C9 and CYP2D6 over 20% without (CYP1A2: 49%) or after a 3-hour preincubation (CYP1A2: 46%, CYP2B6: 43%, CYP2C8: 31%, CYP3A4: 47%). CYP3A4 inhibition by (+)-*N*-3-benzylnirvanol was in line with previously reported data by Suzuki et al. (2002). Inhibition against CYP1A2, CYP2B6, and CYP2C8 was not observed in that study, possibly because of the use of a (+)-*N*-3-benzylnirvanol concentration that was 10-fold lower (Suzuki et al., 2002). Based on the current comparison, we recommend (−)-*N*-3-benzylphenobarbital as a selective chemical inhibitor for CYP2C19 in suspended human hepatocytes over omeprazole and (+)-*N*-3-benzylnirvanol.

Because the main advantage of using human hepatocytes is the presence of the whole complement of phase I and II drug-metabolizing enzymes, the impact of (−)-*N*-3-benzylphenobarbital (1 μM) on AO, FMO3, NAT2, UGT1A1, UGT1A4, UGT2B15, and UGT2B7 was evaluated. (−)-*N*-3-benzylphenobarbital demonstrated less than 10% inhibition of these enzymes, supporting the use of (−)-*N*-3-benzylphenobarbital as a selective CYP2C19 inhibitor in suspended human hepatocytes. In literature, no data are available about (−)-*N*-3-benzylphenobarbital's selectivity against non-CYP enzymes. However, these data are important to support the use of (−)-*N*-3-benzylphenobarbital as a CYP2C19 inhibitor in suspended human hepatocytes.

A set of clinically applied CYP2C19 substrates was used to validate the use of (−)-*N*-3-benzylphenobarbital for the prediction of $fm_{CYP2C19}$. Cl_{int} values were calculated either by following parent depletion or by monitoring metabolite formation. Two tested CYP2C19 substrates, citalopram and moclobemide, were left out of the correlation since turnover was too low to follow parent depletion, and not all of the metabolites could be detected by HRMS. For omeprazole, a lower concentration (0.005 μM) was incubated because omeprazole inhibits its metabolism by 20% at a concentration of 0.5 μM, resulting in an underprediction of the $fm_{CYP2C19}$ (unpublished data).

When the in-house batch of human hepatocytes (BSU) was applied to predict $fm_{CYP2C19}$, it provided a trend toward $fm_{CYP2C19}$ underprediction. Because CYP3A4 is involved in the metabolism of almost all of the tested substrates, a potential hypothesis is that the BSU batch may have an impaired CYP3A4/CYP2C19 activity ratio. Another experiment was performed using a batch of human hepatocytes with lower CYP3A4 activity and similar activity for other major CYP enzymes as compared with the BSU batch (Supplemental Table 3). The results showed the impact of intrinsic CYP activities on fm determination. As expected, the use of the other hepatocyte batch resulted in an increase of the $fm_{CYP2C19}$ for most compounds. Studies indicating that the activities of several CYP enzymes, including CYP3A4, are increased after cryopreservation of human hepatocytes, could support the choice for hepatocyte lots with lower CYP3A4 activity (Smith et al., 2012).

Another possible explanation for the underestimation of $fm_{CYP2C19}$ is that the inhibition potency of (−)-*N*-3-benzylphenobarbital could depend on the substrate used to optimize the experimental conditions. A study by Foti and Wahlstrom (2008) states that the use of different probe substrates for CYP2C19 may result in variable inhibition profiles. They showed that (*S*)-(+)-mephenytoin was the probe substrate that was most sensitive to inhibition (Foti and Wahlstrom, 2008). Therefore, it is possible that some of the clinical substrates are less sensitive to inhibition, resulting in less than 90% inhibition of the CYP2C19 metabolism and a subsequent underprediction of the $fm_{CYP2C19}$.

Besides the in vitro data, the reported in vivo data should also be scrutinized. Most in vivo $fm_{CYP2C19}$ values are based on poor-metabolizer/extensive-metabolizer pharmacokinetics. To our knowledge, no literature data are available on the activity of enzymes other than CYP2C19 in CYP2C19 poor metabolizers. It is possible that the activities of these other enzymes are altered in CYP2C19 poor metabolizers, resulting in a false readout of the true $fm_{CYP2C19}$. However, an increase in the activity of other CYP enzymes would lead to even lower predicted $fm_{CYP2C19}$ values. Furthermore, the in vivo data for some compounds are based on a limited number of subjects, implying that the data could be biased by interindividual variability.

The currently presented in vitro–in vivo $fm_{CYP2C19}$ correlations open the floor for discussion on relevant CYP activities in human hepatocyte batches for phenotyping studies. In the future, additional research is needed to further identify the optimal human hepatocyte batch for fm_{CYP} estimation. In conclusion, this study confirms the selective CYP2C19 inhibition by (−)-*N*-3-benzylphenobarbital in suspended human hepatocytes already demonstrated using liver microsomes supplemented with proof of selectivity against clinically relevant non-CYP enzymes (AO, FMO3, NAT2, UGT1A1, UGT1A4, UGT2B7, and UGT2B15). (−)-*N*-3-Benzylphenobarbital is therefore the preferred CYP2C19 inhibitor to assess $fm_{CYP2C19}$ in suspended human hepatocytes over omeprazole and (+)-*N*-3-benzylnirvanol. In an optimized batch of human hepatocytes, (−)-*N*-3-benzylphenobarbital (1 μM) can be used to accurately assess the in vivo contribution of CYP2C19 to hepatic drug metabolism.

Acknowledgments

The authors would like to acknowledge Oriana Laforgia for her experimental support.

Authorship Contributions

Participated in research design: Cuypers, Chanteux, Ungell, Nicolaï.

Conducted experiments: Cuypers, Gillent, Bonnaillie, Saunders, Beckers, Delatour, Dell'Aiera, Nicolaï.

Performed data analysis: Cuypers, Gillent, Bonnaillie, Saunders, Beckers, Delatour, Dell'Aiera, Nicolaï.

Wrote or contributed to the writing of the manuscript: Cuypers, Chanteux, Gillent, Bonnaillie, Saunders, Beckers, Delatour, Dell'Aiera, Ungell, Nicolaï.

References

Bohnert T, Patel A, Templeton I, Chen Y, Lu C, Lai G, Leung L, Tse S, Einolf HJ, Wang Y-H, et al.; International Consortium for Innovation and Quality in Pharmaceutical Development (IQ) Victim Drug-Drug Interactions Working Group (2016) Evaluation of a new molecular entity as a victim of metabolic drug-drug interactions-an industry perspective. *Drug Metab Dispos* **44**: 1399–1423.

Brandon EF, Raap CD, Meijerman I, Beijnen JH, and Schellens JH (2003) An update on in vitro test methods in human hepatic drug biotransformation research: pros and cons. *Toxicol Appl Pharmacol* **189**:233–246.

Brown HS, Griffin M, and Houston JB (2007) Evaluation of cryopreserved human hepatocytes as an alternative in vitro system to microsomes for the prediction of metabolic clearance. *Drug Metab Dispos* **35**:293–301.

Cai X, Wang RW, Edom RW, Evans DC, Shou M, Rodrigues AD, Liu W, Dean DC, and Baillie TA (2004) Validation of (-)-N-3-benzyl-phenobarbital as a selective inhibitor of CYP2C19 in human liver microsomes. *Drug Metab Dispos* **32**:584–586.

Chai T and Draxler RR (2014) Root mean square error (RMSE) or mean absolute error (MAE)? *Geoscientific Model Development Discussions* **7**:1525–1534.

Chan SW, Hu M, Ko SS, Tam CW, Fok BS, Yin OQ, Chow MS, and Tomlinson B (2013) CYP2C19 genotype has a major influence on labetalol pharmacokinetics in healthy male Chinese subjects. *Eur J Clin Pharmacol* **69**:799–806.

FDA (2020) Guidance for Industry: In Vitro Drug Interaction Studies - Cytochrome, P450, Enzyme- and Transporter-Mediated Drug Interactions. Retrieved from https://www.fda.gov/regulatory-information/search-fda-guidance-documents/vitro-drug-interaction-studies-cytochrome-p450-enzyme-and-transporter-mediated-drug-interactions.

Foti RS and Wahlstrom JL (2008) CYP2C19 inhibition: the impact of substrate probe selection on in vitro inhibition profiles. *Drug Metab Dispos* **36**:523–528.

Gerin B, Dell'Aiera S, Richert L, Smith S, and Chanteux H (2013) Assessment of cytochrome P450 (1A2, 2B6, 2C9 and 3A4) induction in cryopreserved human hepatocytes cultured in 48-well plates using the cocktail strategy. *Xenobiotica* **43**:320–335.

GraphPad (2020) Equation: log(inhibitor) vs. respons - Variable slope. Retrieved from https://www.graphpad.com/guides/prism/7/curve-fitting/reg_dr_inhibit_variable.htm.

Jiang J, Wolters JE, van Breda SG, Kleinjans JC, and de Kok TM (2015) Development of novel tools for the in vitro investigation of drug-induced liver injury. *Expert Opin Drug Metab Toxicol* **11**:1523–1537.

Kazmi F, Sensenhauser C, and Greway T (2019) Characterization of the in vitro inhibitory potential of the oligonucleotide imetelstat on human cytochrome P450 enzymes with predictions of in vivo drug-drug interactions. *Drug Metab Dispos* **47**:9–14.

Khojasteh SC, Prabhu S, Kenny JR, Halladay JS, and Lu AY (2011) Chemical inhibitors of cytochrome P450 isoforms in human liver microsomes: a re-evaluation of P450 isoform selectivity. *Eur J Drug Metab Pharmacokinet* **36**:1–16.

Ko J-W, Sukhova N, Thacker D, Chen P, and Flockhart DA (1997) Evaluation of omeprazole and lansoprazole as inhibitors of cytochrome P450 isoforms. *Drug Metab Dispos* **25**:853–862.

Lindmark B, Lundahl A, Kanebratt KP, Andersson TB, and Isin EM (2018) Human hepatocytes and cytochrome P450-selective inhibitors predict variability in human drug exposure more accurately than human recombinant P450s. *Br J Pharmacol* **175**:2116–2129.

Liu Y, She M, Wu Z, and Dai R (2011) The inhibition study of human UDP-glucuronosyltransferases with cytochrome P450 selective substrates and inhibitors. *J Enzyme Inhib Med Chem* **26**:386–393.

Nelson AC, Huang W, and Moody DE (2001) Variables in human liver microsome preparation: impact on the kinetics of l-α-acetylmethadol (LAAM) n-demethylation and dextromethorphan O-demethylation. *Drug Metab Dispos* **29**:319–325.

Obach RS, Baxter JG, Liston TE, Silber BM, Jones BC, MacIntyre F, Rance DJ, and Wastall P (1997) The prediction of human pharmacokinetic parameters from preclinical and in vitro metabolism data. *J Pharmacol Exp Ther* **283**:46–58.

Parmentier Y, Pothier C, Delmas A, Caradec F, Trancart MM, Guillet F, Bouaita B, Chesne C, Brian Houston J, and Walther B (2017) Direct and quantitative evaluation of the human CYP3A4 contribution (f_m) to drug clearance using the in vitro SILENSOMES model. *Xenobiotica* **47**: 562–575.

Patsalos PN (2013) *Antiepileptic Drug Interactions: A Clinical Guide*, Springer, London.

Sakai T, Aoyama N, Kita T, Sakaeda T, Nishiguchi K, Nishitora Y, Hohda T, Sirasaka D, Tamura T, Tanigawara Y, et al. (2001) CYP2C19 genotype and pharmacokinetics of three proton pump inhibitors in healthy subjects. *Pharm Res* **18**:721–727.

Shirasaka Y, Sager JE, Lutz JD, Davis C, and Isoherranen N (2013) Inhibition of CYP2C19 and CYP3A4 by omeprazole metabolites and their contribution to drug-drug interactions. *Drug Metab Dispos* **41**:1414–1424.

Smith CM, Nolan CK, Edwards MA, Hatfield JB, Stewart TW, Ferguson SS, Lecluyse EL, and Sahi J (2012) A comprehensive evaluation of metabolic activity and intrinsic clearance in suspensions and monolayer cultures of cryopreserved primary human hepatocytes. *J Pharm Sci* **101**: 3989–4002.

Sohn DR, Kusaka M, Ishizaki T, Shin SG, Jang IJ, Shin JG, and Chiba K (1992) Incidence of S-mephenytoin hydroxylation deficiency in a Korean population and the interphenotypic differences in diazepam pharmacokinetics. *Clin Pharmacol Ther* **52**:160–169.

Suzuki H, Kneller MB, Haining RL, Trager WF, and Rettie AE (2002) (+)-N-3-Benzyl-nirvanol and (-)-N-3-benzyl-phenobarbital: new potent and selective in vitro inhibitors of CYP2C19. *Drug Metab Dispos* **30**:235–239.

Tanaka M, Ohkubo T, Otani K, Suzuki A, Kaneko S, Sugawara K, Ryokawa Y, Hakusui H, Yamamori S, and Ishizaki T (1997) Metabolic disposition of pantoprazole, a proton pump inhibitor, in relation to S-mephenytoin 4′-hydroxylation phenotype and genotype. *Clin Pharmacol Ther* **62**:619–628.

Walzer M, Bekersky I, Blum RA, and Tolbert D (2012) Pharmacokinetic drug interactions between clobazam and drugs metabolized by cytochrome P450 isoenzymes. *Pharmacotherapy* **32**: 340–353.

Yao C, Kunze KL, Trager WF, Kharasch ED, and Levy RH (2003) Comparison of in vitro and in vivo inhibition potencies of fluvoxamine toward CYP2C19. *Drug Metab Dispos* **31**:565–571.

Zanger UM and Schwab M (2013) Cytochrome P450 enzymes in drug metabolism: regulation of gene expression, enzyme activities, and impact of genetic variation. *Pharmacol Ther* **138**:103–141.

Address correspondence to: Johan Nicolaï, Development Science, UCB Biopharma SRL, Chemin du Foriest, B-1420 Braine-l'Alleud, Belgium. E-mail: johan.nicolai@ucb.com

SUPPLEMENTARY MATERIAL

Title: (-)-N-3-Benzylphenobarbital is superior to omeprazole and (+)-N-3-benzylnirvanol as a CYP2C19 inhibitor in suspended human hepatocytes

Authors: Marie-Lynn Cuypers[1], Hugues Chanteux[2], Eric Gillent[2], Pierre Bonnaillie[2], Kenneth Saunders[2], Claire Beckers[1], Claude Delatour[2], Sylvie Dell'Aiera[2], Anna-Lena Ungell[2], Johan Nicolaï[2]

Affiliations:

[1]Pharmaceutical Sciences, KU Leuven, Herestraat 49, 3000 Leuven, Belgium.

[2]Development Science, UCB Biopharma SRL, Chemin du Foriest, 1420 Braine-l'Alleud, Belgium.

Journal: Drug metabolism and disposition

Supplemental Table 1. CYP and aldehyde oxidase probe reactions, final substrate concentrations, and cocktail wherein they were used in selectivity experiments of omeprazole, (+)-N-3-benzylnirvanol, and (-)-N-3-benzylphenobarbital.

CYP enzyme	Probe Reaction	Final Substrate Concentration (μM)	Cocktail
1A2	phenacetin O-deethylation	2	1
2B6	bupropion 4-hydroxylation	7	1
2C8	rosiglitazone 5-hydroxylation	5	/
2C9	diclofenac 4-hydroxylation	20	1
2C19	(S)-(+)-mephenytoin 4-hydroxylation	5	2
2D6	dextromethorphan O-demethylation	5	2
3A4	midazolam 1-hydroxylation	5	1
AO	carbazeran 4-hydroxylation	5	/

Supplemental Table 2. M/z transitions of all used UPLC-MS/MS methods.

Substrate	Q1 mass (Da)	Q3 mass (Da)
Cocktail 1		
Phenacetin	180.2	139.9
Acetaminophen	152.2	110.1
Acetaminophen-D_4	156.2	114.0
Bupropion	240.2	184.0
Hydroxybupropion	256.2	139.0
Hydroxybupropion-D_6	262.2	139.1
Diclofenac	296.3	213.9
4-Hydroxydiclofenac	312.0	229.9
4-Hydroxydiclofenac-$^{13}C_6$	318.2	235.9
Midazolam	326.2	223.1
1-Hydroxymidazolam	342.1	203.0
1-Hydroxymidazolam-D_4	346.1	203.0
Cocktail 2		
(S)-(+)-Mephenytoin	219.2	134.0
4-Hydroxymephenytoin	235.0	150.0
4-Hydroxymephenytoin-D_3	238.0	150.0
Dextrometorphan	272.2	171.1
Dextrorphan	258.0	157.0
Dextrorphan-D_3	261.0	157.0
Rosiglitazone	357.0	135.0
5-Hydroxyrosiglitazone	374.0	151.0
5-Hydroxyrosiglitazone-D_4	378.0	151.0
4-Hydroxycarbazeran	377.4	287.9
Monitor parent drug disappearance		
Omeprazole	346.1	198.0
Rabeprazole	360.1	242.0
Lansoprazole	370.1	251.9
Pantoprazole	384.2	200.0
Labetalol	329.2	311.0
(S)-(+)-Mephenytoin	217.0	188.1
Dextrometorphan	272.2	171.1

Supplemental Table 3. In-house comparison (probe reactions Supplemental Table 1) of enzyme activity in HUP182981 and BSU human hepatocytes.

Enzyme	HUP182981	BSU
	Activity (µL/min/million cells)	
CYP1A2	5.53	4.89
CYP2B6	0.77	0.94
CYP2C9	4.77	4.74
CYP2C19	7.42	6.58
CYP2D6	4.36	3.22
CYP3A4	5.70	40.8